Joint Subchannel Allocation and Power Control in Licensed and Unlicensed Spectrum for Multi-Cell UAV-Cellular Network

Amr S. Matar, *Graduate Student Member, IEEE*, and Xuemin Shen, *Fellow, IEEE*

***Abstract*— In this paper, we investigate the resource and interference management problem in a novel scenario where multiple unmanned aerial vehicle base stations (UAV-BSs) provide cellular services to UAV users (UAV-UEs) by reusing both licensed and unlicensed spectrum. Considering the co-existence of terrestrial cellular, WiFi and UAV-BSs, a joint optimization problem is formulated for both subchannel allocation and power control of UAV-UEs over the licensed/unlicensed spectrum in order to maximize the uplink sum-rate of the multi-cell UAV-cellular network. Since the formulated problem is NP-hard, we decompose it into three sub-problems. Specifically, we first use the convex optimization and the Hungarian algorithm to obtain the global optimal of power and subchannel allocations in the licensed spectrum, respectively. Then, we propose a matching game with externalities and coalition game algorithms to obtain the Nash stable of the subchannel allocation in the unlicensed band. Local optimal power assignment in the unlicensed spectrum is obtained using the successive convex approximation (SCA) method. An iterative algorithm is thereby developed to solve the three sub-problems sequentially till reaching convergence. Simulation results show that the proposed algorithm can improve the network capacity by nearly two times than the Long Term Evolution-Advanced (LTE-A).**

***Index Terms*— UAV, unlicensed spectrum, matching game with externalities, interference management.**

I. Introduction

RECENTLY, there is a significant increase in using unmanned aerial vehicles (UAVs) for real-time monitoring, surveillance, precision agriculture, logistics, and enhancing wireless coverage, etc. [1]–[3]. In those applications, a UAV is considered as aerial user equipment, which requires appropriate techniques to ensure highly reliable communication between UAVs and ground stations. As a new type of cellular user, UAV users (UAV-UEs) could produce severe degradation in the overall performance of the terrestrial cellular system [4], [5]. In particular, higher co-channel interference can be obtained due to the line-of-sight (LoS) connection between the destination and interference ground base stations (BSs). Besides, due to the radiation nulls and the down-tilt of the BS antennas [6], UAV-UEs are forced to associate with far BSs if faced one of these nulls, which raises the handover request rate and increase the possibility of handover failure. Therefore, the existing cellular network designed for terrestrial users is not able to readily serve UAV-UEs. Meanwhile, a UAV can also work as a base station (UAV-BS) for providing broadband wireless connectivity during disasters due to its flexible deployment [7], [8]. According to [9], [10], UAV-BSs can be a promising solution to provide reliable wireless connectivity for UAV-UEs. Therefore, the need for a three-dimension (3D) cellular network consisting of both UAV-BSs and UAV-UEs has become essential.

A. Related Works and Motivations

Several works investigated the issues related to integrating the cellular-connected UAVs into the cellular system as a new aerial cellular user equipment [11]–[20]. In [11], an interference-aware path planning scheme was proposed for cellular-connected UAVs which aims to strike a balance between minimizing UAV interference with terrestrial system and maximizing the UAV energy efficiency. In [12], an interference-aware path planning scheme was proposed to minimize the mission completion time of a UAV-UE while maintaining the minimum quality-of-service (QoS) requirement with the ground BSs. The work in [13] jointly optimized the trajectory, operation time, transmit power, and communication scheduling of the UAV-UE to maximize the throughput subject to energy and QoS constraints. In [14], UAV-UEs collaboratively built a global outage probability model in the environment using federated learning (FL) to optimize the UAVs' paths for minimizing the UAV travel time. The UAV coverage probability analysis in the uplink transmission has been introduced in [15]–[17]. In [16], the minimum UAV-UE flying height along a predefined trajectory was determined during a concurrent transmission with a ground cellular user using non-orthogonal multiple access and with a given QoS constraint. In [17], the ground BSs served the cellular-connected UAVs by using the coordinated multi-point (CoMP) transmission. In particular, a framework to derive the lower and upper bound of UAV coverage probability was proposed to measure the effect of speed, altitude, and collaboration distance of the UAV on the achieved performance. In [18], the power allocation and cell association of the UAV

Manuscript received October 15, 2020; revised February 21, 2021; accepted April 11, 2021. Date of publication June 16, 2021; date of current version October 18, 2021. This work was supported by The Bureau of Cultural and Educational Affairs of Egypt in Canada. *(Corresponding author: Amr S. Matar.)*

The authors are with the Department of Electrical and Computer Engineering, University of Waterloo, Waterloo, ON N2L 1W3, Canada (e-mail: asmatar@uwaterloo.ca; sshen@uwaterloo.ca).

Color versions of one or more figures in this article are available at https://doi.org/10.1109/JSAC.2021.3088672.

Digital Object Identifier 10.1109/JSAC.2021.3088672

were jointly optimized to maximize a weighted sum-rate of the UAV-UEs and the ground cellular users in the uplink. In [19], a cooperative interference cancellation approach was introduced for a multi-beam UAV to maximize the uplink sum-rate of the connected BS and, in the meanwhile, mitigate the UAV's uplink interference at each of the other ground BSs. In [20], a novel mechanism was proposed to dynamically tune the down-tilt angles of all the ground BSs for providing efficient mobility support to the UAVs moving in the sky through maximizing the received signal power while also maintaining good throughput performance of the ground users. However, the prior studies only focus on investigating the trajectory and coverage probability of cellular-connected UAV without involving the UAV-BS to serve the UAV-UEs for reducing the impact of severe UAV-UE interference on the ground cellular network.

As an extension of the cellular network to serve terrestrial users, the deployment and trajectory design of UAV-BSs have attracted high attention recently. The authors in [21] proposed a multi-agent reinforcement learning framework to optimize the resource allocation, such that each UAV-BS can adjust its resource, power, and associated users separately without exchanging information among them. The joint design of UAV-BS trajectory and resource allocation was proposed in [22], [23] to maximize the network throughput while considering the ground cellular users' fairness through using deep reinforcement learning algorithms. In [24], the UAV-BS placement, user association, and resource allocation were jointly considered by designing an iterative algorithm to maximize the ground cellular users' throughput and achieve fairness among them. In [25], a UAV-BS equipped with a millimetre-wave (mmWave) multiple-input multiple-output (MIMO) antenna was deployed to provide wireless access to IoT devices from different clusters in the downlink transmission. The authors jointly optimized transmit power, beam pattern, and 3D placement of the UAV-BS to maximize the system's downlink sum-rate.

The use of LTE in the unlicensed spectrum, *a.k.a* LTE-U, with UAV-BS was introduced in [26], [27]. In [26], the authors formulated a problem that jointly optimizes user association, content caching, and spectrum allocation of a UAV-BS that serves ground cellular users over the LTE licensed and unlicensed spectrum. A game for load balancing between UAV-BSs and WiFi access points in the unlicensed band was proposed in [27] to verify a sufficient throughput for all users. However, providing LTE service for cellular-connected UAVs in the unlicensed spectrum to fulfil their high demand data rate has not been considered yet.

Recently, a few articles investigated the performance of using the UAV-BS to provide cellular service to the UAV-UEs. The authors in [9] proposed a 3D placement algorithm for a UAV-BS equipped with a directional antenna to maximize the number of covered UAV-UEs subject to a given spectrum sharing policy with the terrestrial network. In [28], UAV-to-UAV (U2U) pairs sharing the same uplink band of ground cellular users are assumed, where the coverage probability and rate are evaluated under two spectrum sharing mechanisms through an analytical framework that considers channel models, antenna patterns, and practical power control schemes. For the Underlay mechanism, results showed that U2U communications might have a limited harmful effect on the ground user uplink performance since BSs receive the UAV power signals through their antenna sidelobes. A novel 3D fully-fledged UAV-cellular network was introduced in [10], where a framework was proposed to solve the two essential problems of 3D cell association and network planning.

However, none of these previous works [9]–[28] studied the joint resource and interference management for multi-cell UAV-cellular network which reuses both licensed and unlicensed band.

B. Research Contributions

The main contribution of this paper is that we propose a novel UAV cellular network allowing UAV-BSs to effectively serve UAV-UEs in uplink transmission through both licensed and unlicensed spectrum. We propose a joint resource and interference management scheme over the licensed/unlicensed bands to guarantee the coexistence of the cellular/WiFi systems, respectively. In particular, interference threshold protection for both cellular and WiFi networks, as well as the inter-cell interference (ICI) between UAV-BSs in the unlicensed band, are considered. To our best knowledge, this is the first work that considers using LTE in both licensed and unlicensed spectrum for multi-cell UAV-cellular network under the joint coexistence guarantee with both cellular and WiFi networks, respectively. Our key research contributions include:

- This work investigates reusing both licensed and unlicensed spectrum besides considering the multi-cell case for a UAV-cellular network. We formulate a joint subchannel allocation and power control optimization problem in licensed/unlicensed band aiming to maximize the uplink sum-rate of the system subject to the QoS constraint of UAV-UEs and the inter-cell interference.
- We consider mutual interference threshold protection constraints in the licensed/unlicensed band to ensure the harmonious coexistence of our proposed system concurrently with the cellular/WiFi networks, respectively.
- We decompose the formulated NP-hard optimization problem into three sub-problems. First, we use the convex optimization and Hungarian algorithm to get the global optimum power and subchannel allocations in the licensed spectrum, respectively. By using the obtained results from the previous sub-problem, secondly, the Nash-stable subchannel allocations in the unlicensed spectrum are reached using a matching game with externalities and coalition game algorithms. Third, we use the successive convex approximation technique to obtain the local optimum power values in the unlicensed band. Finally, an iterative algorithm is proposed to solve the optimization problem iteratively till it converges.
- We compare the proposed algorithm with three various schemes in the simulation. The results show that the proposed algorithm outperforms the greedy algorithm by about 15.7% in terms of the network uplink sum-rate.

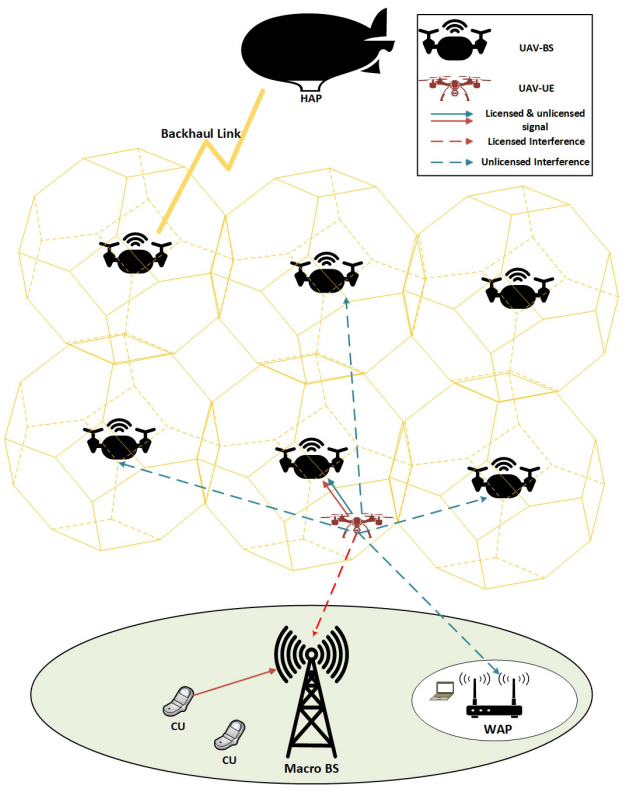

Fig. 1. LTE-U UAV-Cellualr network system model.

Moreover, the proposed algorithm can improve the system capacity to more than double the LTE-A scheme.

The remainder of this paper is organized as follows. The UAV-cellular network system model is presented in Section II. In Section III, we formulate and jointly solve the resource allocation and power control optimization problem. In Section IV, we analyze the computational complexity of the proposed algorithm. Simulation results are presented and analyzed in Section V. Finally, conclusions are summarized in Section VI.

II. System Model

A. Scenario Description

Consider a 3D UAV-Cellular network as shown in Fig.1, which is composed of M UAV-BSs, denoted by the set $\mathcal{M}$, N UAV-UEs, and a number of High Altitude Platform (HAP) UAVs which provide the wireless backhaul connectivity for the UAV-BSs. In this system, each UAV-BS $j \in \mathcal{M}$ serves a set of $\mathcal{N}_j$ UAV-UEs in the uplink transmission. Therefore, the set of the total number of UAV-UEs are $\mathcal{N} = \bigcup_{j\in\mathcal{M}} \mathcal{N}_j$. We also consider a single cell cellular network that consists of a BS located at $(0, 0, H_{BS})$ and a number of ground cellular users (CUs). In addition, we assume that there are W non-overlapping WiFi Access Points (WAPs).

We assume that an orthogonal set of finite licensed subchannels C_j^L with uniform bandwidth B_L has been allocated to UAV-BS j. Hence, UAV-BS $j \in \mathcal{M}$ assigns enough resources from the licensed band for each UAV-UE $i \in \mathcal{N}_j$ to retain a predefined uplink data rate of $R_{i,j}^{Licensed}$. For reliable control signal transmission from UAV-UE to UAV-BS, each UAV-UE is only allowed to access one licensed subchannel, and each licensed subchannel is assigned to at most one UAV-UE at each UAV-BS. In addition, the UAV-BSs and UAV-UEs can reinforce the uplink data rate through operating in the unlicensed radio spectrum in order to support a minimum transmission data rate of $QoS_{i,j}, \forall i \in \mathcal{N}, \forall j \in \mathcal{M}$. The bandwidth B_c of the unlicensed channel c is divided by the UAV-cellular system into a set of finite subchannels C^U with uniform bandwidth B_U for efficient resource management. To obtain the highest spectrum efficiency, a frequency reuse factor equal to one in the unlicensed spectrum has been considered. In other words, We assume each UAV-BS $j \in \mathcal{M}$ can use all the unlicensed band to serve its UAV-UEs in the uplink transmission. Thus, each UAV-BS is affected by interference from $M-1$ UAV-BSs and one WAP, whereas one WAP experiences interference from M UAV-BSs.

As in [10], a 3D space can be filled completely using an arrangement of truncated octahedron structure cells where at the center of each cell, a UAV-BS has been placed. Each structure consists of 14 faces with 6 square and 8 regular hexagonal shapes. The 3D locations of these UAV-BSs can be determined using:

$$L_{a,b,c} = [x_0, y_0, z_o] + \sqrt{2}R[a+b-c, \\ -a+b+c, a-b+c], \quad (1)$$

where $[x_0, y_0, z_o]$ is the Cartesian coordinates of a given reference location (e.g. the center of the 3D space), a, b, c are integers chosen from set $\{\ldots, -2, -1, 0, 1, 2, \ldots\}$, and R is the edge length of the considered truncated octahedron. After the locations of UAV-BSs have been obtained, these locations will not change within a time slot. In contrast, the UAV-UE can move freely with a speed of $[0, v_{max}]$ in any time slot.[1] The time slot is chosen to be sufficiently small such that the UAV-UEs' locations can be assumed to be approximately constant within each time slot duration even at maximum UAV-UE's speed as commonly done in the literature [11], [29].

The location of UAV-UE $i \in \mathcal{N}$ in time slot t is denoted as (x_i^t, y_i^t, z_i^t), and the UAV-BS $j \in \mathcal{M}$ is located at (x_j, y_j, z_j) which have been obtained from equation (1). Therefore, in time slot t, the distance between UAV-UE i and UAV-BS j is calculated as

$$d_{i,j}^t = \sqrt{(x_i^t - x_j)^2 + (y_i^t - y_j)^2 + (z_i^t - z_j)^2}, \quad (2)$$

B. Data Transmission Model

1) Data Rate in the Licensed Spectrum: When a UAV-BS $j \in \mathcal{M}$ assigns to UAV-UE $i \in \mathcal{N}_j$ a subchannel $k \in C_j^L$, the achieved rate of that user in time slot t is

$$R_{i,j}^{Licensed} = B_L \log_2\left(1 + \frac{\psi_{i,j}^{k,t} P_{i,j}^{k,t} g_{i,j}^{k,t}}{\sigma^2}\right). \quad (3)$$

where σ^2 is the noise power, $g_{i,j}^{k,t}$ is the free-space channel gain between UAV-UE i and UAV-BS j over subchannel k, and $P_{i,j}^{k,t}$ is the transmit power from UAV-UE i to UAV-BS j

[1] In this paper, we add the superscript t to some notations to distinguish the fixed parameters from the time-varying parameters.

over licensed subchannel k. The binary variable $\psi_{i,j}^{k,t} = \{0,1\}$ represents the subchannel allocation of the licensed subchannel k between UAV-UE i and UAV-BS j. We define the licensed subchannels allocation matrix as $\Psi = \left[\psi_{i,j}^{k,t}\right]_{N\times M\times C_j^L}$, where $\psi_{i,j}^{k,t} = 1$ means that subchannel $k \in C_j^L$ is assigned to UAV-UE $i \in \mathcal{N}_j$, and $\psi_{i,j}^{k,t} = 0$ otherwise. The ground CU uplink interference on UAV-BS j is negligible due to the high elevation angle, fading, and shadowing.

2) Data Rate in the Unlicensed Spectrum: When a UAV-BS $j \in \mathcal{M}$ assigns to UAV-UE $i \in \mathcal{N}_j$ a subchannel $q \in C^U$ from the unlicensed spectrum, the achieved rate of that user in time slot t is

$$R_{i,j}^{Unlicensed,q} = B_U \log_2\left(1 + \frac{\phi_{i,j}^{q,t} P_{i,j}^{q,t} g_{i,j}^{q,t}}{I_{UAV,j}^{q,t} + \sigma^2}\right), \tag{4}$$

where the binary variable $\phi_{i,j}^{q,t} = \{0,1\}$ represents the subchannel allocation between UAV-UE i and UAV-BS j over subchannel q, such that $\phi_{i,j}^{q,t} = 1$ means that the subchannel q is assigned to UAV-UE i, and $\psi_{i,j}^{q,t} = 0$ otherwise. $P_{i,j}^{q,t}$ is the transmit power from UAV-UE i to UAV-BS j over unlicensed subchannel q. We define $\Phi = \left[\phi_{i,j}^{q,t}\right]_{N\times M\times C^U}$ and $P_U = \left[P_{i,j}^{q,t}\right]_{N\times M\times C^U}$ as unlicensed subchannels and transmission power allocation matrices, respectively. $I_{UAV,j}^{q,t}$ is the inter-cell interference at UAV-BS j over subchannel q during time slot t, which can be expressed as

$$I_{UAV,j}^{q,t} = \sum_{y\in M\setminus y\neq j} \sum_{x\in\mathcal{N}_y} \phi_{x,y}^{q,t} P_{x,y}^{q,t} g_{x,j}^{q,t}. \tag{5}$$

where $\sum_{y\in M\setminus y\neq j} \sum_{x\in\mathcal{N}_y}$ means the sum of the interference from all UAV-UEs that use subchannel q in all the interfering UAV-BSs. The WAP co-channel interference on UAV-BS j is negligible due to the high elevation angle, the wall penetration loss, and the low transmit power of WAP.

If UAV-BS j assigns more than one subchannel to UAV-UE i, then the total achieved rate of that user from the unlicensed band in time slot t is

$$R_{i,j}^{Unlicensed} = \sum_{q\in C^U} \phi_{i,j}^{q,t} R_{i,j}^{Unlicensed,q}. \tag{6}$$

3) UAV-UE QoS: A minimum data rate ($QoS_{i,j}$) is required by each UAV-UE for its applications. When $R_{i,j}^{Licensed} \leq QoS_{i,j}$, each UAV-BS j allows its UAV-UE i to access resources from the unlicensed spectrum to enhance UAV-UE's data rate. Thus, The QoS requirement for UAV-UE i is achieved through the following constraint:

$$R_{i,j} = R_{i,j}^{Licensed} + R_{i,j}^{Unlicensed} \geq QoS_{i,j}. \tag{7}$$

C. Interference Threshold Protection

1) For Cellular System: We use the Air-to-Ground (A2G) pathloss model between LAP UAV-UE and cellular BS which has been proposed in [30], [31]. In time slot t, the average A2G pathloss from UAV-UE i and BS in dB can be expressed as

$$PL_{i,BS}^{avg,t} = 20\log\left(\frac{4\pi f_c^L}{c}\right) + 20\log\left(d_{i,BS}^t\right) + P_{LoS,i}^t \eta_{LoS} + \left(1 - P_{LoS,i}^t\right)\eta_{NLoS}, \tag{8}$$

where f_c^L is the carrier frequency of licensed band, c is the speed of light, $d_{i,BS}^t$ is the distance between UAV-UE i and the cellular BS, η_{LoS} and η_{NLoS} are the average additional losses for LoS and NLoS links, respectively, which depend on environment, and $P_{LoS,i}^t$ is the LoS probability of A2G link which can be denoted as

$$P_{LoS,i}^t = \frac{1}{1 + a\exp(-b(\theta_i^t - a))}, \tag{9}$$

where a and b are environmental dependent constants, and $\theta_i^t = sin^{-1}\left(\left(z_i^t - H_{BS}\right)/d_{i,BS}^t\right)$ is the elevation angle.

In our system model, reusing the same licensed spectrum leads to mutual interference between the UAV-cellular network and the terrestrial network. Therefore, in order to ensure the coexistence between the two systems, it is assumed that the total interference introduced from UAV-UEs to the cellular BS on subchannel $k \in C_j^L$ does not exceed a given threshold $I_{Licensed}^{th,k}$, i.e.,

$$\sum_{i\in\mathcal{N}_j} \psi_{i,j}^{k,t} \frac{P_{i,j}^{k,t}}{10^{PL_{i,BS}^{avg,t}/10}} \leq I_{Licensed}^{th,k}, \quad \forall j \in \mathcal{M},\ \forall k \in C_j^L. \tag{10}$$

2) For WiFi System: The A2G pathloss model [30] is also considered, where the average pathloss from UAV-UE i to WAP in time slot t can be expressed as

$$PL_{i,WAP}^{avg}(t) = 20\log\left(\frac{4\pi f_c^U}{c}\right) + 20\log\left(d_{i,WAP}^t\right) + P_{LoS,i}^t \eta_{LoS} + \left(1 - P_{LoS,i}^t\right)\eta_{NLoS} + \rho, \tag{11}$$

where f_c^U is the carrier frequency of unlicensed band, $d_{i,WAP}^t$ is the distance between UAV-UE i and the WAP, ρ is the wall penetration loss, and the other parameters can be derived from equations (8)-(9).

The non-orthogonality between LTE and WAP respective transmitted signals leads to mutual interference due to the coexistence on the same unlicensed spectrum. Based on [32] and [33], the interference at WAP introduced by the transmission of UAV-UE $i \in \mathcal{N}_j$ on subchannel q can be determined as

$$I_{i,WAP}^q = \int_{d_q - /B_c/2}^{d_q + B_c/2} \frac{P_{i,j}^{q,t}}{10^{PL_{i,WAP}^{avg,t}/10}} T_s \left(\frac{sin\ \pi f T_s}{\pi f T_s}\right)^2 df, \tag{12}$$

where d_q represents the spectral distance between subchannel q and WAP occupied band B_c, and T_s is the OFDM symbol duration.

We assume that the UAV-cellular network can utilize the unlicensed band c as long as the total interference initiated from all UAV-UEs to the WAP does not exceed $I_{Unlicensed}^{th,B_c}$

$$\sum_{j\in\mathcal{M}} \sum_{i\in\mathcal{N}_j} \sum_{q\in C^U} \phi_{i,j}^{q,t} P_{i,j}^{q,t} O_{i,j}^{q,t} \leq I_{Unlicensed}^{th,B_c}, \tag{13}$$

where

$$O_{i,j}^{q,t} = \frac{1}{10^{PL_{i,WAP}^{avg,t}/10}} \int_{d_q - B_c/2}^{d_q + B_c/2} T_s \left(\frac{sin\ \pi f T_s}{\pi f T_s}\right)^2 df. \tag{14}$$

III. Joint Subchannel Allocation and Power Control

In this section, first, we formulate the joint subchannel allocation and power control optimization problem. Then, we propose an iterative solution for the problem after decomposing it into three sub-problems and solve each of them with the appropriate approach.

A. Problem Formulation

Since the UAV-cellular network is uplink dominant, the uplink sum-rate of this network is one key metric to evaluate the performance of this network. We aim to maximize the uplink sum-rate of the UAV-UEs for the multi-cell UAV-cellular network by jointly optimizing the subchannel allocation and power control variables in both licensed and unlicensed spectrum ($\Psi, P_L, \Phi, and\ P_U$). We formulate the optimization problem as follows:

$$
\begin{aligned}
&\max_{(\Psi,P_L,\Phi,P_U)} \sum_{j\in\mathcal{M}}\sum_{i\in\mathcal{N}_j} R_{i,j},\\
&s.t.,\ C_1: R_{i,j} \geq QoS_{i,j}, \quad \forall j\in\mathcal{M},\ \forall i\in\mathcal{N}_j\\
&\quad C_2: \sum_{i\in\mathcal{N}_j} \psi_{i,j}^{k,t} \frac{P_{i,j}^{k,t}}{10^{PL_{i,BS}^{avg,t}/10}} \leq I_{Licensed}^{th,k},\\
&\quad \forall j\in\mathcal{M}, \quad \forall k\in C_j^L\\
&\quad C_3: \sum_{j\in\mathcal{M}}\sum_{i\in\mathcal{N}_j}\sum_{q\in\mathcal{C}^U} \phi_{i,j}^{q,t} P_{i,j}^{q,t} O_{i,j}^{q,t} \leq I_{Unlicensed}^{th,B_c}\\
&\quad C_4: \sum_{i\in\mathcal{N}_j}\sum_{k\in C_j^L} \psi_{i,j}^{k,t} \leq C_j^L, \quad \forall j\in\mathcal{M}\\
&\quad C_5: \sum_{i\in\mathcal{N}_j} \psi_{i,j}^{k,t} \leq 1, \quad \forall j\in\mathcal{M},\ \forall k\in C_j^L\\
&\quad C_6: \sum_{k\in C_j^L} \psi_{i,j}^{k,t} \leq 1, \quad \forall j\in\mathcal{M},\ \forall i\in\mathcal{N}_j\\
&\quad C_7: \sum_{i\in\mathcal{N}_j}\sum_{q\in C^U} \phi_{i,j}^{q,t} \leq C^U,\ \forall j\in\mathcal{M}\\
&\quad C_8: \sum_{i\in\mathcal{N}_j} \phi_{i,j}^{q,t} \leq 1, \quad \forall j\in\mathcal{M},\ \forall q\in C^U\\
&\quad C_9: \psi_{i,j}^{k,t} = \{0,1\}, \quad \forall j\in\mathcal{M},\ \forall i\in\mathcal{N}_j,\ \forall k\in C_j^L\\
&\quad C_{10}: \phi_{i,j}^{q,t} = \{0,1\}, \quad \forall j\in\mathcal{M},\ \forall i\in\mathcal{N}_j,\ \forall q\in C^U\\
&\quad C_{11}: P_{i,j}^{k,t} \leq P_{max}^{k}, \quad \forall j\in\mathcal{M},\ \forall i\in\mathcal{N}_j,\ \forall k\in C_j^L\\
&\quad C_{12}: P_{i,j}^{q,t} \leq P_{max}^{q}, \quad \forall j\in\mathcal{M},\ \forall i\in\mathcal{N}_j,\ \forall q\in C^U
\end{aligned}
\tag{15}
$$

The minimum QoS rate requirement for UAV-UEs is achieved through constraint (C_1). The coexistence with both terrestrial cellular and WiFi systems are secured through constraints (C_2) and (C_3), respectively. Constraints (C_5) and (C_8) guarantee that each licensed and unlicensed subchannel are allocated to at most one UAV-UE per UAV-BS, while constraint (C_6) ensures that each UAV-UE can be assigned to at most one licensed subchannel. The limitation of total licensed/unlicensed subchannels per UAV-BS is represented by constraints (C_4)/(C_7), respectively. The transmit power of each UAV-UE on both licensed and unlicensed subchannels must be within the permitted range of the total transmitted power on each subchannel as shown in constraints (C_{11}) and (C_{12}), respectively.

The optimization problem in (15) is a non-convex Mixed Integer Non-Linear Programming (MINLP) optimization problem which is NP-hard to solve in general. The non-convexity is imputed for two reasons. The first one is the combinatorial nature of licensed and unlicensed subchannel allocation binary variables (Ψ, Φ). The second one is due to the ICI equation in both objective function and constraint (C_1). In the following theorem, we prove that the optimization problem (15) is NP-hard.

Theorem 1: Problem (15) is NP-hard.

Proof: See Appendix A. ■

B. Sub-Optimal Problem Decomposition

Since problem (15) is NP-hard, to solve this problem efficiently, we decompose it into three sub-problems, i.e. licensed subchannel allocation and power control, unlicensed subchannel allocation, and power control over unlicensed band sub-problems. First, the licensed resource allocation and power control sub-problem can be expressed as follow:

$$
\begin{aligned}
&\max_{(\Psi,P_L)} \sum_{j\in\mathcal{M}}\sum_{i\in\mathcal{N}_j} R_{i,j}^{Licensed}\\
&s.t.\ C_2, C_4, C_5, C_6, C_9, C_{11}.
\end{aligned}
\tag{16}
$$

Given the subchannel Ψ and power P_L allocation matrices in the licensed band (achieved data rate from the licensed spectrum) obtained from (16), the subchannel allocation sub-problem and the power control sub-problem in the unlicensed band can be represented as follow:

$$
\begin{aligned}
&\max_{\Phi} \sum_{j\in\mathcal{M}}\sum_{i\in\mathcal{N}_j} R_{i,j}^{Unlicensed}\\
&s.t.\ C_1, C_3, C_7, C_8, C_{10}.
\end{aligned}
\tag{17}
$$

and

$$
\begin{aligned}
&\max_{P_U} \sum_{j\in\mathcal{M}}\sum_{i\in\mathcal{N}_j} R_{i,j}^{Unlicensed}\\
&s.t.\ C_1, C_3, C_{12}.
\end{aligned}
\tag{18}
$$

Sub-problems (17) and (18) have the same objective function with different constraints and variables. The solution of sub-problem (17) can be used to solve the sub-problem (18), and vice versa repeatedly until converge. We use a matching game with externalities and a coalition formation game to solve sub-problem (17) and successive convex approximation (SCA) method for sub-problem (18). This solution approach is shown in Fig. 2. The details of these approaches are represented in the following subsections.

C. Subchannel Allocation and Power Control in the Licensed Band Sub-Problem

In this subsection, we give a detailed description of the sub-problem (16) solution. Since there is no ICI among UAV-BSs in the licensed spectrum, we can decompose sub-problem (16)

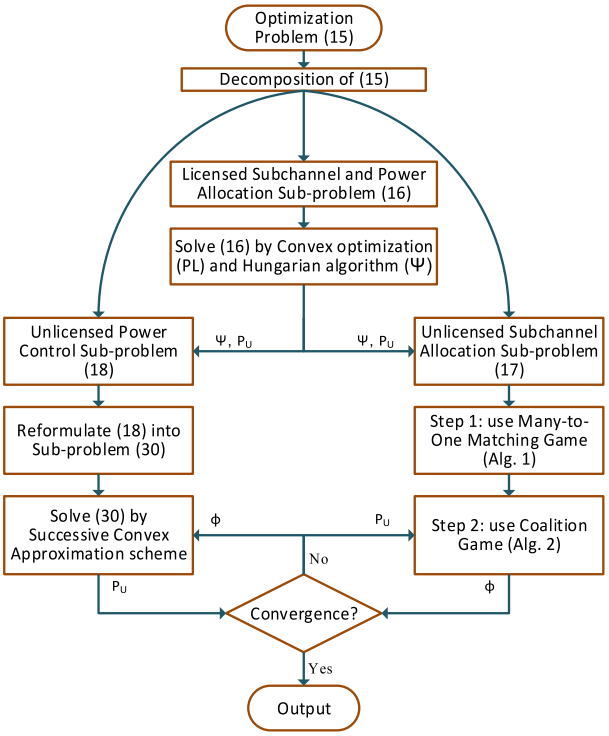

Fig. 2. Solution process of the problem (15).

into M distributed sub-problems in which each one is solved based on the solution below at each UAV-BS independently. Each sub-problem is a combinatorial optimization problem concerning Ψ for a fixed P_L. Additionally, it is a concave function with respect to $P_{i,j}^{k,t}$ for a given Ψ. The optimum subchannel allocation and power control in the licensed band can be found by solving two sub-sub-problems iteratively as follows.

1) *power control phase:* For a given Ψ, each sub-problem is concave with respect to P_L. Therefore, the optimal power allocation can be determined based on the KKT conditions [34].
2) *subchannel allocation phase:* For a given P_L, the sub-problem is combinatorial in the variable Ψ, where the Hungarian method [35] is used to obtain the optimal subchannel allocations.

D. Unlicensed Subchannel Allocation Sub-Problem

In this subsection, we propose a solution for sub-problem (17) by using a many-to-one matching game with externalities and a coalition formation game.

1) Matching Game: The unlicensed subchannel allocation sub-problem shown in (17) is still NP-hard and cannot be efficiently solved. Therefore, we propose a matching game as introduced in Alg. 1 to solve this sub-problem. The intuition of this matching game is to allocate the unlicensed subchannels in such a way that maximize the uplink sum-rate of the UAV-cellular network while satisfying the QoS requirements of UAV-UE. Thus, lines 3-5 are responsible for calculating the QoS gap for UAV-UEs connected to UAV-BS j between the achieved data rate from the licensed subchannel and the QoS

Algorithm 1 Unlicensed Subchannel Allocation for UAV-BS j

1: Input : QoS, $R^{Licensed}$, P_U, N_j, $\Phi_j^{initial}$
2: Output : Φ_j
3: **for** each $i \in \mathcal{N}_j$ **do**
4: Calculate QoS gap by $QG_{i,j} = [QoS_{i,j} - R_{i,j}^{Licensed}]^+$
5: **end for**
6: Sort UAV-UEs from $\mathcal{N}_j$ according to channel gain on descending order
7: Reorder the elements of QG_j according to $\mathcal{N}_j$
8: **for** each subchannel $q \in C^U$ **do**
9: Calculate the ICI on each subchannel using eq. (5)
10: **end for**
11: Sort subchannels from C^U according to ICI on each subchannel on ascending order
12: Set $q = 1$
13: **for** each $i \in \mathcal{N}_j$ **do**
14: Set $RqBW = QG_{i,j}$
15: **if** $RqBW \neq 0$ **then**
16: **while** $RqBW > 0$ **do**
17: Set $\phi_{i,j}^q = 1$
18: Calculate $R_{i,j}^{Unlicensed,q}$ using eq. (6)
19: Set $RqBW = RqBW - R_{i,j}^{Unlicensed,q}$
20: Set $q = q + 1$
21: **end while**
22: **end if**
23: **end for**

requirement. Line 6 sorts UAV-UEs as the descending order based on their channel gain, and line 7 reorder the elements of the QoS gap vector according to the sorted UAV-UE list. After that, in lines 8-11, ICI is calculated on each unlicensed subchannel and then sort subchannels in ascending order based on the ICI calculated. Finally, lines 12-23 are responsible for allocating the unlicensed subchannels with the least ICI values based on the list obtained from line 11 to the UAV-UE list obtained from line 6 while satisfying the QoS gap of each UAV-UE according to the list given from line 7.

Due to the ICI, a subchannel selection by a UAV-UE is affected by the other UAV-UEs choices for the same sub-channel. This is known as the externalities, where traditional preference orders cannot solve it. Therefore, we formulated a coalition matching game as follows to cope with these externalities.

2) Coalition Game: The unlicensed subchannel allocation problem is modeled as a coalitional game to acquire the network utility in terms of the network uplink sum-rate. For each binary parameter $\phi_{i,j}^q = 1$, there is a formed access link between UAV-BS $j \in \mathcal{M}$ and UAV-UE $i \in \mathcal{N}$ on unlicensed subchannel $q \in C^U$. Therefore, for each unlicensed subchannel $q \in C^U$, there is a maximum M simultaneous access link use this channel through the network since we considered the frequency reuse factor is equal to one.

For the unlicensed subchannel allocation, the game players are the links. We have $\mathcal{L}$ links where each link defined by $j \in \mathcal{M}, i \in \mathcal{N}, q \in C^U$. S_q is the coalition of the links occupying

the same subchannel $q \in C^U$. Since there are C^U unlicensed subchannels in the network, the links can be divided into C^U coalitions at most with the following restrictions:

$$\mathcal{L} = S_1 \cup S_2 \cup \ldots \cup S_{C^U}, \quad S_q \cap S_k = \emptyset, \times \forall q,\ k \in C^U \ and\ q \neq k. \quad (19)$$

The coalition utility function $U(S_q)$ is defined as the sum rate of all links in coalition S_q, which given by

$$U(S_q) = \sum_{j \in \mathcal{M}} \sum_{i \in \mathcal{N}_j} R_{i,j}^{Unlicensed,q}. \quad (20)$$

Since the utility is proportional to the network sum-rate, links tend to form coalitions of different subchannels to maximize the coalitional game utility. Therefore, the game formation definitions are defined based on the content above as follows:

- *Players*: The set of access links is denoted as $\mathcal{L}$.
- *Coalition*: The set of players $\mathcal{L}$ is divided into $|C^U|$ coalitions, according to restrictions given in (19).
- *Utility*: $U(S_q)$ is the uplink sum-rate value for each coalition $U(S_q) \subseteq \mathcal{L}$, which is a transferable utility for members in S_q.
- *Strategy*: Players decide to enter or depart a coalition according to the results of the utility comparison between original and new coalition.

Definition 1 (The coalition partition): A coalitional partition is defined as the set $\Theta = \{S_1, \ldots, S_p\}\,(1 \leq p \leq |C^U|)$, which partitions the players set $\mathcal{L}$, i.e., $\forall p, S_c \subseteq \mathcal{L}$ are disjoint coalitions such that $\bigcup_{c=1}^{p} S_c = \mathcal{L}$.

In order to maximize the network throughput, preference relation for players to decide whether to join or leave a coalition should be well defined. Instead of initial partition $\Theta = \{S_1, \ldots, S_p\}$, a group of players prefers to adopt the utilitarian order to organize themselves into a collection of coalitions $\tilde{\Theta} = \{\tilde{S}_1, \ldots, \tilde{S}_p\}$, which is proposed in [36], [37]. Then the utility relationship between two different partitions can be expressed as

$$\sum_{i=1}^{\tilde{p}} U(\tilde{S}_i) > \sum_{i=1}^{p} U(S_i) \quad (21)$$

Definition 2 (Total utility of coalitions): For a partition $\Theta = \{S_1, \ldots, S_p\}(1 \leq p \leq |C^U|)$, of the set $\mathcal{L}$, the total utility can be calculated as:

$$U(\Theta) = \sum_{i=1}^{p} U(S_i). \quad (22)$$

If $U(\tilde{\Theta}) > U(\Theta)$, the partition $\tilde{\Theta}$ has a better performance on total utility. Every coalition in $\tilde{\Theta}$ is the coalition of links which share the same sub-channel. The total utility here is total uplink sum throughput of the network over unlicensed spectrum.

Definition 3 (Preference relation $\succ_l$): For any player l, a preference relation $\succ_l$ is defined as a complete, reflexive, and transitive binary relation over the set of all coalitions that player l may form.

Switch rule 1: for any players $l, l' \in \mathcal{L}, l \in S_p, l' \in S_q, S_p \neq S_q, i' \neq i, j' = j$, players l and l' strictly prefer to switch their coalition with each other ($S_q \succ_l S_p$ and $S_p \succ_{l'} S_q$) when preference relation satisfies

$$U(\{\{S_p \setminus l\} \cup l'\}) + U(\{\{S_q \setminus l'\} \cup l\}) > U(S_p) + U(S_q), \quad S_p,\ S_q \subseteq \mathcal{L},\ S_p \neq S_q, \quad (23)$$

then the partition Θ is modified into a new partition as follows

$$\Theta = (\Theta \setminus \{S_p, S_q\}) \cup \{\{S_p \setminus l\} \cup l'\} \cup \{\{S_q \setminus l'\} \cup l\}. \quad (24)$$

Switch rule 2: for any players $l \in \mathcal{L}, l \in S_p$, player l strictly prefers to switch its coalition from S_p to coalition S_q ($S_q \succ_l S_p$), $S_q \neq S_p, \forall l' \in S_q, \nexists i' = i, \nexists j' = j$, where preference relation can be defined as follows

$$U(\{S_p \setminus l\}) + U(\{S_q \cup l\}) > U(S_p) + U(S_q), \times S_p, S_q \subseteq \mathcal{L}, S_p \neq S_q. \quad (25)$$

then the partition Θ is modified into a new partition as follows

$$\Theta = (\Theta \setminus \{S_p, S_q\}) \cup \{S_p \setminus l\} \cup \{S_q \cup l\}. \quad (26)$$

Algorithm 2 Coalition Formation Algorithm for Unlicensed Subchannel Allocation

1: Input : The partition Θ from the previous algorithm
2: Output : Final Nash-stable partition Θ_{final}
3: **while** Nash-stable partition is not achieved **do**
4: Randomly choose a link $l \in \mathcal{L}$, and denote its current coalition as $S_p \in \Theta$;
5: Randomly choose another coalition $S_q \in \Theta,\ S_q \neq S_p$;
6: **if** S_q has a link $l' \in \mathcal{L}, i' = i, j' = j$ **then**
7: Set $S_{\overline{q}} = S_q$;
8: Randomly choose another coalition $S_q \in \Theta$, $S_q \neq S_{\overline{q}},\ S_q \neq S_p$;
9: Go back to line 6;
10: **else if** S_q has a link $l' \in \mathcal{L}, i' \neq i, j' = j$ **then**
11: **if** rule satisfies ($S_q \succ_l S_p$ and $S_p \succ_{l'} S_q$) **then**
12: $\Theta = (\Theta \setminus \{S_p, S_q\}) \cup \{\{S_p \setminus l\} \cup l'\} \cup \{\{S_q \setminus l'\} \cup l\}$;
13: **else**
14: Set $S_{\overline{q}} = S_q$;
15: Randomly choose another coalition $S_q \in \Theta$, $S_q \neq S_{\overline{q}},\ S_q \neq S_p$;
16: Go back to line 6;
17: **end if**
18: **else**
19: **if** rule satisfies ($S_q \succ_l S_p$) **then**
20: $\Theta = (\Theta \setminus \{S_p, S_q\}) \cup \{S_p \setminus l\} \cup \{S_q \cup l\}$;
21: **end if**
22: **end if**
23: **end while**

Based on these definitions and switching rules, the coalition formation game pseudo code is shown in Algorithm 2. As shown in line 3-23, the coalition formation algorithm performs the judgment to determine whether to perform a switch operation based on definition (3). In line 10-17, when there is a link l' inside the selected coalition (S_q) for the same UAV-BS but different UAV-UE, the first coalition switch

operation judgment shown in switch rule 1 is examined. If the switch operation satisfies switch rule 1, the switch operation is performed, and the algorithm ends this round of loops and repeats the above operations. If the first switch operation judgment does not meet the switch rule 1, it selects a different coalition S_q and continues examining switch rules. Similarly, in lines 18-22, if there is no any link inside coalition S_q for the same UAV-BS, it examines switch rule 2, and if switch rule 2 is satisfied, it performs the switch operation.

Theorem 2: The final partition Θ_{final} in coalition formation game algorithm is Nash-stable.

Proof. See Appendix B. ■

E. Unlicensed Power Control Sub-Problem

The power control sub-problem (18) in the unlicensed spectrum is still a non-convex problem owing to the ICI coupling between cells. To solve this sub-problem, we use the successive convex approximation (SCA) approach. SCA method can obtain a solution that satisfies the KKT conditions of the original non-convex problem through approximating it by a series of convex approximations [38]. Thus, we solve the convex approximation problem starting from the initial point and then using the output solution as an initial point for the new convex problem till it converges to a solution that satisfies the KKT conditions of the original non-convex problem. The SCA algorithm is guaranteed to converge after multiple iterations [39].

We first introduce the auxiliary variable $P_{i,j}^{q,t} = e^{\overline{P_{i,j}^{q,t}}}$. Therefore, the sub-problem (18) can be reduced to the following:

$$\begin{aligned}
&\max_{\overline{P_U}} \sum_{j\in\mathcal{M}}\sum_{i\in\mathcal{N}_j}\sum_{q\in C^U} \phi_{i,j}^{q,t}\log_2(1+\gamma_{i,j}^{q,t}),\\
&s.t., \sum_{q\in C^U} \phi_{i,j}^{q,t} B_U \log_2(1+\gamma_{i,j}^{q,t})\\
&\quad \geq \left[QoS_{i,j} - R_{i,j}^{Licensed}\right]^+, \quad \forall j,\ \forall i,\\
&\quad \sum_{j\in\mathcal{M}}\sum_{i\in\mathcal{N}_j}\sum_{q\in\mathcal{C}^U} \phi_{i,j}^{q,t} e^{\overline{P_{i,j}^{q,t}}} O_{i,j}^{q,t} \leq I_{Unlicensed}^{th,B_c},\\
&\quad \overline{P_{i,j}^{q,t}} \leq \ln(P_{max}^q), \quad \forall j\in\mathcal{M},\ \forall i\in\mathcal{N}_j,\ \forall q\in C^U.
\end{aligned} \tag{27}$$

where the intermediate variable is given by the following:

$$\gamma_{i,j}^{q,t} = \frac{e^{\overline{P_{i,j}^{q,t}}} g_{i,j}^{q,t}}{\sum_{y\in M\setminus y\neq j}\sum_{x\in\mathcal{N}_y} \phi_{x,y}^{q,t} e^{\overline{P_{x,y}^{q,t}}} g_{x,j}^{q,t} + \sigma^2}. \tag{28}$$

The objective function and the first constraint are still non-convex. However, from [40] the lower bound of $f(x) = \log(1+x)$ is given by $\hat{f}(x) = \xi\log x + \upsilon$, where $\xi = \frac{x}{1+x}$ and $\upsilon = \log(1+x) - \frac{x}{1+x}\log(x)$. This lower bound satisfies the following conditions:

$$\begin{aligned}
\hat{f}(x) &< f(x),\\
\hat{f}(x_0) &= f(x_0),\\
\frac{\partial\hat{f}(x)}{x}\,|_{x_0} &= \frac{\partial f(x)}{x}\,|_{x_0}\,.
\end{aligned} \tag{29}$$

Therefore, the sub-problem (27) is reformulated to the following:

$$\begin{aligned}
&\max_{\overline{P_U}} \sum_{j\in\mathcal{M}}\sum_{i\in\mathcal{N}_j}\sum_{q\in C^U} \phi_{i,j}^{q,t}[\xi_{i,j}^{q,t}\log_2(\gamma_{i,j}^{q,t}) + \upsilon_{i,j}^{q,t}],\\
&s.t., \sum_{q\in C^U} \phi_{i,j}^{q,t}[\xi_{i,j}^{q,t}\log_2(\gamma_{i,j}^{q,t}) + \upsilon_{i,j}^{q,t}]\\
&\quad \geq \left[QoS_{i,j} - R_{i,j}^{Licensed}\right]^+,\\
&\quad \sum_{j\in\mathcal{M}}\sum_{i\in\mathcal{N}_j}\sum_{q\in\mathcal{C}^U} \phi_{i,j}^{q,t} e^{\overline{P_{i,j}^{q,t}}} O_{i,j}^{q,t} \leq I_{Unlicensed}^{th,B_c},\\
&\quad \overline{P_{i,j}^{q,t}} \leq \ln(P_{max}^q), \quad \forall j\in\mathcal{M},\ \forall i\in\mathcal{N}_j,\ \forall q\in C^U.
\end{aligned} \tag{30}$$

Theorem 3: Problem (30) is a convex optimization problem.

Proof: We examine the convexity of objective function and the first constraint. Since $\log_2(\gamma_{i,j}^{q,t})$ can be rearranged as follow:

$$\begin{aligned}
\log_2(\gamma_{i,j}^{q,t}) = \frac{\ln(\gamma_{i,j}^{q,t})}{\ln(2)} = \frac{1}{\ln(2)}\Big(&\ln(g_{i,j}^{q,t}) + \overline{P_{i,j}^{q,t}}\\
&- \ln\Big(\sum_{y\in M\setminus y\neq j}\sum_{x\in\mathcal{N}_y} \phi_{x,y}^{q,t} e^{\overline{P_{x,y}^{q,t}}} g_{x,j}^{q,t} + \sigma^2\Big)\Big)
\end{aligned} \tag{31}$$

From above equation, $\log_2(\gamma_{i,j}^{q,t})$ is concave because the log-sum-exponential function is convex [34]. The objective function and the first constraint are combination of concave functions. Therefore, the power control sub-problem in the unlicensed spectrum is a convex optimization problem. ■

F. Iterative Licensed/Unlicensed Subchannel Allocation and Power Control Algorithm

In this subsection, we introduce an iterative algorithm to solve the optimization problem (15), where the three sub-problems are solved iteratively until convergence. The process of the iterative algorithm is summarized in Algorithm 3.

Theorem 4: Algorithm 3 is guaranteed to converge.

Algorithm 3 Iterative Licensed/Unlicensed Subchannel Allocation and Power Control Algorithm

1: Initialization: $\mathcal{N}$, $\mathcal{M}$, C_j^L, C^U, QoS
2: **Step 1:** solve sub-problem (16) in order to get the global optimum of licensed subchannel Ψ and power P_L allocations, and calculate the global optimum $R^{Licensed}$.
3: **Step 2:** use algorithm 1 to allocate unlicensed subchannel to UAV-UEs based on the QoS requirement.
4: **repeat**
5: **Step 3: Coalition Game**: use algorithm 2 to reach Nash-stable unlicensed subchannel allocation.
6: **Step 4: Successive Convex Approximation**: solve sub-problem (30) until convergence.
7: **until** Convergence
8: Output: Ψ, P_L, Φ, P_U

Proof: Algorithm 3 first calculates the optimal global allocations of both subchannels and power in the licensed spectrum. After that, each iteration of Algorithm 3 comprises two sub-problems, the coalition game sub-problem and the SCA sub-problem. In Theorem 2, we argued that the coalition game would reach a Nash-stable partition. In addition, the SCA algorithm guarantees to converge to a local optimum solution that is very close to the global optimum [38]. Since the network uplink sum-rate is improved in each iteration and there is an upper bound for the uplink sum-rate, Algorithm 3 is guaranteed to converge in a limited number of iterations. ■

IV. Computational Complexity Analysis

In the proposed algorithm, the sub-problem (16) is solved first to find the global optimum of power and subchannel in the licensed spectrum. An iterative method has been introduced in which the power assignment sub-problem is solved directly with convex problem solutions, and the subchannel allocation sub-problem is solved efficiently by the Hungarian algorithm. Since the computation of the sub-problem (16) is distributed to each UAV-BS, the computational complexity for step 1 of Algorithm 3 is $\mathcal{O}(K_1 \times (\mathcal{N}_m C_m^L)^3)$ [35], where K_1 is a constant equivalent to the number of iteration which is very small due to the convexity and the linear programming nature of the power and subchannel allocation sub-problems, respectively.

For the subchannel allocation sub-problem in the unlicensed spectrum, Algorithm 1 (a many-to-one matching game) is used at each UAV-BS to provide UAV-UE with initial subchannel allocations. the complexity of this algorithm is $\mathcal{O}(\mathcal{N}_m \cdot C^U)$ [41]. In Algorithm 2, a coalition game is used to solve the matching game's externalities due to the unlicensed spectrum reuse, where the selection of a subchannel in a cell affects the data rate of all the UAV-UEs in the other cells that use the same subchannel. According to the coalition game, the maximum number of links is $|\mathcal{M}|\cdot|C^U|$. By considering the worst-case scenario, each link is examined with $|C^U - 1|$ coalitions. Therefore, the complexity of Algorithm 2 is $\mathcal{O}(\mathcal{M}(C^U)^2)$. The exhaustive search algorithm can also be used to obtain the optimal subchannel allocation in the unlicensed band. However, the computation complexity of the optimal algorithm is $\mathcal{O}(\mathcal{N}_m^{|\mathcal{M}|\cdot|C^U|})$, which is significantly higher than that of the proposed algorithm.

Finally, the power allocation sub-problem in (30) is a convex optimization problem that CVX can efficiently solve. SCA is iteratively solved (30) by updating the points of interest up to convergence. The SCA algorithm will be run at most $\mathcal{O}(\mathcal{N})$ times [38]. Therefore, the computational complexity for the proposed algorithm is $\mathcal{O}(K_1 \times (\mathcal{N}_m C_m^L)^3 + (\mathcal{N}_m C^U) + K_2 \times (\mathcal{M}(C^U)^2 + \mathcal{N}))$, where K_2 is a constant for the number of times the coalition game and the SCA algorithm will run up to convergence which is finite.

V. Simulation Results

In the simulation, we consider a 3D space of size 2.5km $\times$ 2.5km $\times$ 2.5km, in which the locations of the UAV-UEs are uniformly distributed. The centre point of the 3D space is located 1.4km above the surface ground. The simulation parameters are listed in Table I. We compare our proposed algorithm with three other algorithms: greedy, random allocation, and LTE-A. We calculate the global optimum licensed subchannel and power allocation for the first two algorithms by solving sub-problem one. Then, for the greedy algorithm, we utilize Algorithm 1 in which the unlicensed subchannel allocation uses a greedy algorithm, that UAV-UE always selects subchannels in its preference list with the highest utility. For the random allocation algorithm, the unlicensed subchannel allocation is chosen randomly. The last one is the classical LTE-A scheme, where the UAV-BS serves the UAV-UEs in the licensed spectrum only.

TABLE I
Parameters Values

Parameter	Description	Value
$\mathcal{M}$	Number of LAP UAV-BSs	9
R	Truncated octahedron edge length	400 m
H_{BS}	Height of ground cellular BS	50 m
C_j^L	Number of licensed subchannels	10
C^U	Number of unlicensed subchannels	50
QoS	UAV-UE minimum data rate	4 Mbps
f_c^L	Carrier frequency of licensed band	2 GHz
f_c^U	Carrier frequency of unlicensed band	5 GHz
P_{max}^k	Transmit power on licensed subch.	0.5 Watt
P_{max}^q	Transmit power on unlicensed subch.	0.5 Watt
B_c	Bandwidth of unlicensed channel c	20 MHz
B_L	Licensed subchannel bandwidth	180 KHz
B_U	Unlicensed subchannel bandwidth	180 KHz
σ^2	Noise variance	-114 dBm
η_{LoS}	A2G channel parameter	1 dB
η_{NloS}	A2G channel parameter	20 dB
a	A2G channel parameter	12
b	A2G channel parameter	0.135
ρ	Wall penetration loss	10 dB
$I_{Licensed}^{th,k}$	Interference threshold at cellular BS	-75 dBm
$I_{Unlicensed}^{th,B_c}$	Interference threshold at WAP	-75 dBm

Fig. 3 shows the total uplink sum-rate of the network achieved by different schemes as a function of the number of UAV-UEs per cell. We can note that the overall sum-rate increases as the number of UAV-UEs increases. Fig. 3 shows that when the number of UAV-UEs per cell (n) is between two and three, both the proposed and the greedy algorithms have the same performance, which is slightly better than the LTE-A scheme. The reason for that is, with the low value of n and the availability of the unlicensed spectrum, the two schemes can distribute the unlicensed subchannels among UAV-UEs while maintaining the value of the ICI approximating to zero. However, when the value of n increases from 4 to 10, the ICI turns to be significant; our proposed algorithm achieves nearly 15.7% and 8% improvement in the performance over the other schemes for the low and high level of interference environment,

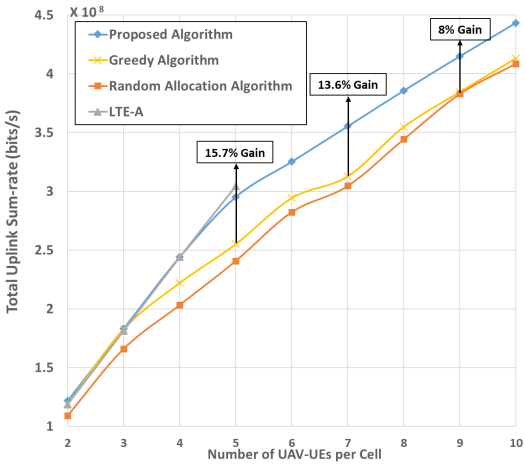

Fig. 3. Total uplink sum-rate as the number of UAV-UEs per cell varies.

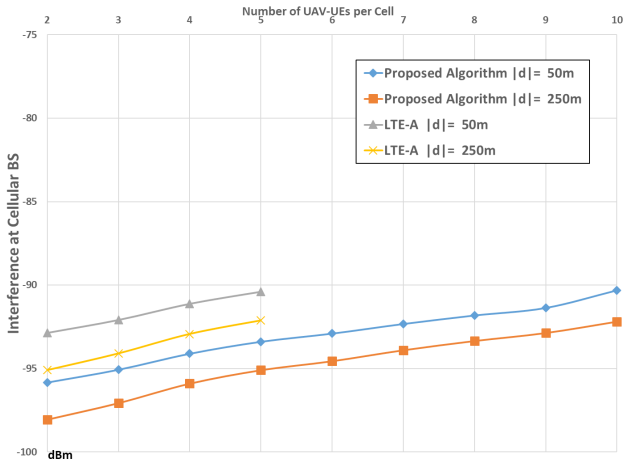

Fig. 5. Interference value at the cellular BS for different schemes in the licensed spectrum vs. n (number of UAV-UEs per cell).

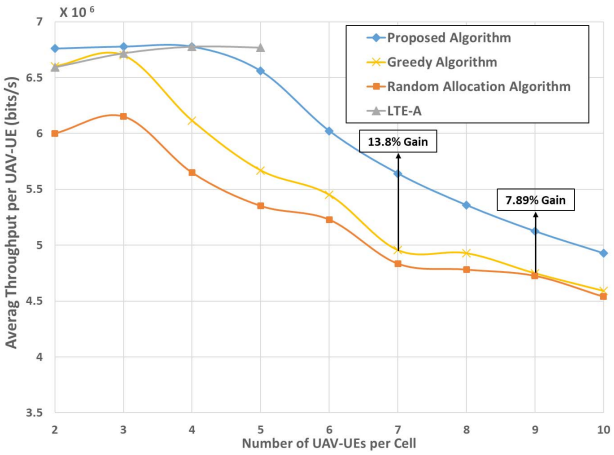

Fig. 4. Average throughput per UAV-UE for different schemes vs. n (number of UAV-UEs per cell).

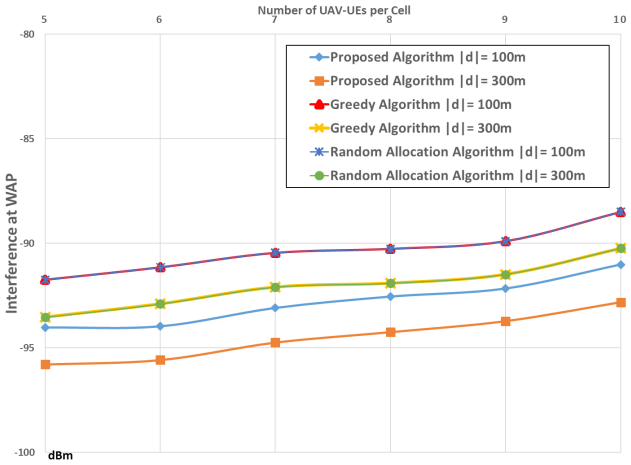

Fig. 6. Interference value at the WAP for different schemes in the unlicensed spectrum vs. n (number of UAV-UEs per cell).

respectively. We also can see that as interference increases, the greedy and random allocation algorithms approximately give the same performance. Moreover, from Fig. 3, we can see that the LTE-A can serve only up to five UAV-UEs per cell, while our proposed algorithm can effectively increase the capacity of the network up to ten UAV-UEs per cell.

Fig. 4 shows the performance of average throughput per UAV-UE for different algorithms. When the value of n is low, the average throughput per UAV-UE for the proposed algorithm is slightly better due to sufficient unlicensed spectrum and ICI absence. Nevertheless, when the value of n equals 5, the LTE-A gives a better performance than the others. In other words, the average throughput achieved using the other schemes decreases as the number of UAV-UEs increases. The reason for that is because as the number of UAV-UEs increases, the ICI value also increases, causing a decrease in the achieved average throughput. However, our proposed algorithm achieves significantly higher performance than the other algorithms. Moreover, the proposed algorithm can double the cell capacity compared to LTE-A while guaranteeing the QoS requirements of the UAV-UEs.

Fig. 5 shows the UAV-cellular network's interference level on the cellular BS for different numbers of UAV-UEs at two different distances between the cellular BS and the lower level of the 3D UAV-cellular network coverage. Since the greedy and random allocation algorithms use the optimum global allocations in the licensed spectrum, which give the same performance as our proposed algorithm in the licensed spectrum, we compare only the proposed algorithm with the LTE-A. As shown in the figure, the proposed algorithm's interference level on cellular BS for the two different distances is significantly lower than the interference level from LTE-A. Besides, the interference level for the two schemes is much less than the interference threshold level. This is because of the orthogonal distribution of the licensed spectrum among the UAV-BSs, making the UAV-UEs produce low interference per subchannel at the cellular BS.

Fig. 6 compares the interference level at a WAP for the proposed, greedy, and random allocation algorithms at two different distances between the WAP and the lower level of the 3D UAV-cellular network coverage. The figure shows that the interference level at the WAP increases as the number of UAV-UEs increases since the WAP is affected by all the

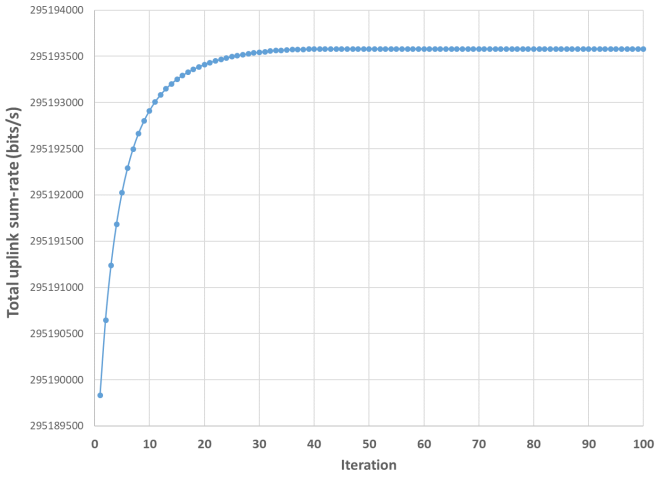

Fig. 7. Convergence of algorithm 3.

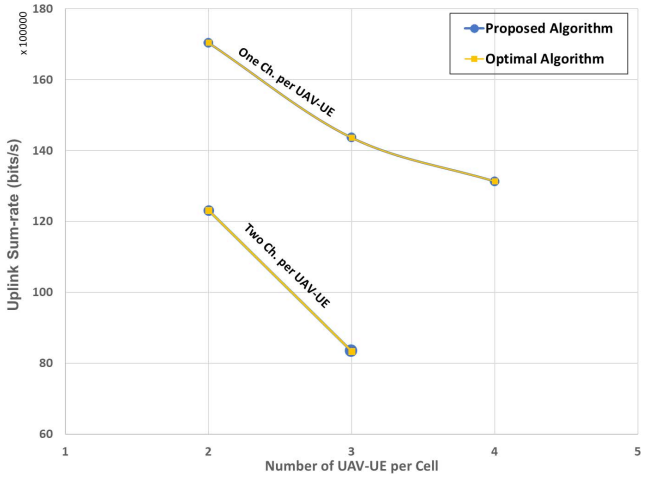

Fig. 8. Comparison with the optimal algorithm.

system's cells, which reuse the entire unlicensed band. The greedy and random allocation schemes produce the same interference levels at the unlicensed band for the different distances since they do not use power control. Again, the proposed algorithm produces significantly lower interference levels over the other schemes for all the different distances. The interference level in the unlicensed spectrum is much less than the threshold level because of the high elevation angle between WAP and UAV-UEs and the wall penetration factor.

Fig. 7 shows the convergence of Algorithm 3 that is used to find the local optimal subchannel and power allocation in both licensed and unlicensed spectrum by iteratively solving (15). As seen in the figure, Algorithm 3 converges after a finite number of iterations.

In Fig. 8, we show that the matching game with externalities and coalition game proposed in Algorithms 1 and 2 reach a Nash-stable solution. Therefore, we use the brute force algorithm to find the optimal subchannel allocation for given power allocation and compare it with the result of the proposed algorithm. Due to the large searching space, we test it for a small network ($\mathcal{M} = 3$, $C^U = 6$ $R_{licensed} = 0$). Fig. 8 shows that Algorithms 1 and 2 give the same optimal uplink sum-rate value as the optimal algorithm.

VI. Conclusion

In this paper, we have presented the uplink sum-rate maximization problem for a novel multi-cell UAV-cellular network. To solve this non-convex NP-hard problem, we proposed an algorithm that solves three sub-problems iteratively. For subchannel and power allocation sub-problem in the licensed spectrum, we obtained the global optimum allocations through using convex optimization and Hungarian algorithm. For the subchannel allocation sub-problem in the unlicensed spectrum, we have proposed a matching game with externalities and a coalition game to reach a Nash-stable solution while considering the inter-cell interference. For the power control sub-problem in the unlicensed band, the success convex approximation method was applied to obtain the local optimal power allocation. In this complex interference network with two different types of interference, our work can offer a significant improvement in the system performance in terms of the network capacity and the overall uplink sum-rate. The problem for multi-operator UAV-cellular networks in the unlicensed spectrum, where inter-operator interference between operators becomes dominant, is left for our future work.

Appendix A
Proof of Theorem 1

Proof: In this appendix, we prove that optimization problem (15) is NP-hard even when we do not consider the licensed band. We construct a simple case of problem (15) where there are only two UAV-BSs in which each unlicensed subchannel can serve one UAV-UE from each cell simultaneously. let $\mathcal{N}_1$, $\mathcal{N}_2$, and $\mathcal{C}$ be three disjoint sets of UAV-UEs per cell one, UAV-UEs per cell two, and unlicensed subchannels, respectively, with $|\mathcal{N}_1| = |\mathcal{N}_2| = |\mathcal{C}|$. Set $\mathcal{N}_1$, $\mathcal{N}_2$, and $\mathcal{C}$ satisfy $\mathcal{N}_1 \cap \mathcal{N}_2 = \emptyset$, $\mathcal{N}_1 \cap \mathcal{C} = \emptyset$, and $\mathcal{N}_2 \cap \mathcal{C} = \emptyset$. Let $\mathcal{P}$ be a collection of ordered triples $\mathcal{P} \subseteq \mathcal{N}_1 \times \mathcal{N}_2 \times \mathcal{C}$, where each element in $\mathcal{P}$ consists a UAV-UE from cell 1, a UAV-UE from cell 2, and an unlicensed subchannel. There exists $\overline{P} \subseteq \mathcal{P}$ that for any two distinct triples $(\mathcal{N}_{1,i}, \mathcal{N}_{2,i}, \mathcal{C}_i) \in \overline{P}$ and $(\mathcal{N}_{1,j}, \mathcal{N}_{2,j}, \mathcal{C}_j) \in \overline{P}$, we have $i \neq j$. Therefore, $\overline{P}$ is a three-dimension matching (3-DM) which has been proved to be NP-complete [42]. Moreover, optimization problem (15) is $(\mathcal{M}+1)$-dimension matching which is more complicated than the 3-DM problem. Therefore, the problem in (15) is NP-hard [29]. ■

Appendix B
Proof of Theorem 2

Proof: In this appendix, we prove that the final partition Θ_{final} in the coalition game algorithm is Nash-stable. If the final partition Θ_{final} is not Nash-stable. Thus, there must exist:

- Two players $l \in S_p, l' \in S_q, S_p \neq S_q (S_p, S_q \subseteq \Theta_{final})$ such that $S_q \succ_l S_p$ and $S_p \succ_{l'} S_q$. or
- A player $l \in S_p (S_p \subseteq \Theta_{final})$ and another coalition $S_q \in \Theta_{final}$ such that $S_q \succ_l S_p$.

Based on our proposed algorithm, for any of the two cases, player l will perform a switch operation with the other player l' or to the available coalition forming a new partition,

which conflicts with the fact that Θ_{final} is the final partition. Therefore, the hypothesis that the final partition Θ_{final} is Nash-stable has been proved. ■

ACKNOWLEDGMENT

The authors would like to thank Prof. Mahmoud M. Elmesalawy and Dr. Weisen Shi for their beneficial suggestions while conducting this work.

REFERENCES

[1] B. Li, Z. Fei, and Y. Zhang, "UAV communications for 5G and beyond: Recent advances and future trends," *IEEE Internet Things J.*, vol. 6, no. 2, pp. 2241–2263, Apr. 2019.

[2] D. Mishra and E. Natalizio, "A survey on cellular-connected UAVs: Design challenges, enabling 5G/B5G innovations, and experimental advancements," *Comput. Netw.*, vol. 182, Dec. 2020, Art. no. 107451.

[3] N. Cheng *et al.*, "Air-ground integrated mobile edge networks: Architecture, challenges, and opportunities," *IEEE Commun. Mag.*, vol. 56, no. 8, pp. 26–32, Aug. 2018.

[4] *Technical Specification Group Radio Access Network; Study on Enhanced LTE Support for Aerial Vehicles (Release 15)*, document GTR 36.777, 3GPP, Dec. 2017.

[5] M. M. Azari, F. Rosas, and S. Pollin, "Cellular connectivity for UAVs: Network modeling, performance analysis, and design guidelines," *IEEE Trans. Wireless Commun.*, vol. 18, no. 7, pp. 3366–3381, Jul. 2019.

[6] M. M. U. Chowdhury, P. Sinha, and I. Güvenç, "Handover-count based velocity estimation of cellular-connected UAVs," in *Proc. IEEE 21st Int. Workshop Signal Process. Adv. Wireless Commun. (SPAWC)*, May 2020, pp. 1–5.

[7] W. Shi *et al.*, "Multi-drone 3-D trajectory planning and scheduling in drone-assisted radio access networks," *IEEE Trans. Veh. Technol.*, vol. 68, no. 8, pp. 8145–8158, Aug. 2019.

[8] N. Cheng *et al.*, "A comprehensive simulation platform for space-air-ground integrated network," *IEEE Wireless Commun.*, vol. 27, no. 1, pp. 178–185, Feb. 2020.

[9] N. Cherif, W. Jaafar, H. Yanikomeroglu, and A. Yongacoglu, "On the optimal 3D placement of a UAV base station for maximal coverage of UAV users," Aug. 2020, *arXiv:2008.09262*. [Online]. Available: http://arxiv.org/abs/2008.09262

[10] M. Mozaffari, A. T. Z. Kasgari, W. Saad, M. Bennis, and M. Debbah, "Beyond 5G with UAVs: Foundations of a 3D wireless cellular network," *IEEE Trans. Wireless Commun.*, vol. 18, no. 1, pp. 357–372, Jan. 2019.

[11] U. Challita, W. Saad, and C. Bettstetter, "Interference management for cellular-connected UAVs: A deep reinforcement learning approach," *IEEE Trans. Wireless Commun.*, vol. 18, no. 4, pp. 2125–2140, Apr. 2019.

[12] S. Zhang, Y. Zeng, and R. Zhang, "Cellular-enabled UAV communication: A connectivity-constrained trajectory optimization perspective," *IEEE Trans. Commun.*, vol. 67, no. 3, pp. 2580–2604, Mar. 2019.

[13] C. Zhan and Y. Zeng, "Energy-efficient data uploading for cellular-connected UAV systems," *IEEE Trans. Wireless Commun.*, vol. 19, no. 11, pp. 7279–7292, Nov. 2020.

[14] B. Khamidehi and E. S. Sousa, "Federated learning for cellular-connected UAVs: Radio mapping and path planning," Aug. 2020, *arXiv:2008.10054*. [Online]. Available: http://arxiv.org/abs/2008.10054

[15] J. Lyu and R. Zhang, "Network-connected UAV: 3-D system modeling and coverage performance analysis," *IEEE Internet Things J.*, vol. 6, no. 4, pp. 7048–7060, Aug. 2019.

[16] N. Senadhira, S. Durrani, X. Zhou, N. Yang, and M. Ding, "Uplink NOMA for cellular-connected UAV: Impact of UAV trajectories and altitude," *IEEE Trans. Commun.*, vol. 68, no. 8, pp. 5242–5258, Aug. 2020.

[17] R. Amer, W. Saad, and N. Marchetti, "Mobility in the sky: Performance and mobility analysis for cellular-connected UAVs," *IEEE Trans. Commun.*, vol. 68, no. 5, pp. 3229–3246, May 2020.

[18] W. Mei, Q. Wu, and R. Zhang, "Cellular-connected UAV: Uplink association, power control and interference coordination," *IEEE Trans. Wireless Commun.*, vol. 18, no. 11, pp. 5380–5393, Nov. 2019.

[19] L. Liu, S. Zhang, and R. Zhang, "Multi-beam UAV communication in cellular uplink: Cooperative interference cancellation and sum-rate maximization," *IEEE Trans. Wireless Commun.*, vol. 18, no. 10, pp. 4679–4691, Oct. 2019.

[20] M. M. U. Chowdhury, W. Saad, and I. Güvenç, "Mobility management for cellular-connected UAVs: A learning-based approach," in *Proc. IEEE Int. Conf. Commun. Workshops (ICC Workshops)*, Jun. 2020, pp. 1–6.

[21] J. Cui, Y. Liu, and A. Nallanathan, "Multi-agent reinforcement learning-based resource allocation for UAV networks," *IEEE Trans. Wireless Commun.*, vol. 19, no. 2, pp. 729–743, Feb. 2020.

[22] W. Shi, J. Li, H. Wu, C. Zhou, N. Cheng, and X. Shen, "Drone-cell trajectory planning and resource allocation for highly mobile networks: A hierarchical DRL approach," *IEEE Internet Things J.*, vol. 8, no. 12, pp. 9800–9813, Jun. 2021.

[23] R. Ding, F. Gao, and X. S. Shen, "3D UAV trajectory design and frequency band allocation for energy-efficient and fair communication: A deep reinforcement learning approach," *IEEE Trans. Wireless Commun.*, vol. 19, no. 12, pp. 7796–7809, Dec. 2020.

[24] C. Qiu, Z. Wei, X. Yuan, Z. Feng, and P. Zhang, "Multiple UAV-mounted base station placement and user association with joint fronthaul and backhaul optimization," *IEEE Trans. Commun.*, vol. 68, no. 9, pp. 5864–5877, Sep. 2020.

[25] W. Feng *et al.*, "Joint 3D trajectory and power optimization for UAV-aided mmWave MIMO-NOMA networks," *IEEE Trans. Commun.*, vol. 69, no. 4, pp. 2346–2358, Apr. 2021.

[26] M. Chen, W. Saad, and C. Yin, "Liquid state machine learning for resource and cache management in LTE-U unmanned aerial vehicle (UAV) networks," *IEEE Trans. Wireless Commun.*, vol. 18, no. 3, pp. 1504–1517, Mar. 2019.

[27] D. Athukoralage, I. Guvenc, W. Saad, and M. Bennis, "Regret based learning for UAV assisted LTE-U/WiFi public safety networks," in *Proc. IEEE Global Commun. Conf. (GLOBECOM)*, Dec. 2016, pp. 1–7.

[28] M. M. Azari, G. Geraci, A. Garcia-Rodriguez, and S. Pollin, "UAV-to-UAV communications in cellular networks," *IEEE Trans. Wireless Commun.*, vol. 19, no. 9, pp. 6130–6144, Sep. 2020.

[29] S. Zhang, H. Zhang, B. Di, and L. Song, "Cellular UAV-to-X communications: Design and optimization for multi-UAV networks," *IEEE Trans. Wireless Commun.*, vol. 18, no. 2, pp. 1346–1359, Feb. 2019.

[30] A. Al-Hourani, S. Kandeepan, and A. Jamalipour, "Modeling air-to-ground path loss for low altitude platforms in urban environments," in *Proc. IEEE Global Commun. Conf.*, Dec. 2014, pp. 2898–2904.

[31] A. Al-Hourani, S. Kandeepan, and S. Lardner, "Optimal LAP altitude for maximum coverage," *IEEE Wireless Commun. Lett.*, vol. 3, no. 6, pp. 569–572, Dec. 2014.

[32] W. Xu, B. Li, Y. Xu, and J. Lin, "Lower-complexity power allocation for LTE-U systems: A successive cap-limited waterfilling method," in *Proc. IEEE 81st Veh. Technol. Conf. (VTC Spring)*, May 2015, pp. 1–6.

[33] T. LeAnh, N. H. Tran, D. T. Ngo, Z. Han, and C. S. Hong, "Orchestrating resource management in LTE-unlicensed systems with backhaul link constraints," *IEEE Trans. Wireless Commun.*, vol. 18, no. 2, pp. 1360–1375, Feb. 2019.

[34] S. Boyd, S. P. Boyd, and L. Vandenberghe, *Convex Optimization*. Cambridge, U.K.: Cambridge Univ. Press, 2004.

[35] H. W. Kuhn, "The Hungarian method for the assignment problem," *Nav. Res. Logistics Quart.*, vol. 2, nos. 1–2, pp. 83–97, Mar. 1955.

[36] M. A. Alim, T. Pan, M. T. Thai, and W. Saad, "Leveraging social communities for optimizing cellular device-to-device communications," *IEEE Trans. Wireless Commun.*, vol. 16, no. 1, pp. 551–564, Jan. 2017.

[37] W. Saad, Z. Han, M. Debbah, A. Hjorungnes, and T. Basar, "Coalitional game theory for communication networks," *IEEE Signal Process. Mag.*, vol. 26, no. 5, pp. 77–97, Sep. 2009.

[38] A. Abdelnasser and E. Hossain, "Resource allocation for an OFDMA cloud-RAN of small cells underlaying a macrocell," *IEEE Trans. Mobile Comput.*, vol. 15, no. 11, pp. 2837–2850, Nov. 2016.

[39] B. R. Marks and G. P. Wright, "A general inner approximation algorithm for nonconvex mathematical programs," *Oper. Res.*, vol. 26, no. 4, pp. 681–683, Aug. 1978.

[40] M. Sami and J. N. Daigle, "User association and power control for UAV-enabled cellular networks," *IEEE Wireless Commun. Lett.*, vol. 9, no. 3, pp. 267–270, Mar. 2020.

[41] M. W. Baidas, M. S. Bahbahani, E. Alsusa, K. A. Hamdi, and Z. Ding, "Joint D2D group association and channel assignment in uplink multi-cell NOMA networks: A matching-theoretic approach," *IEEE Trans. Commun.*, vol. 67, no. 12, pp. 8771–8785, Dec. 2019.

[42] D. S. Johnson and M. R. Garey, *Computers and Intractability: A Guide to the Theory of NP-Completeness*. New York, NY, USA: W. H. Freeman, 1979.

Amr S. Matar (Graduate Student Member, IEEE) received the B.Sc. and M.Sc. degrees from Helwan University, Cairo, Egypt, in 2007 and 2013, respectively. He is currently pursuing the Ph.D. degree with the Department of Electrical and Computer Engineering, University of Waterloo, Canada. His research interests include resource and interference management in the mobile satellite systems and beyond 5G networks.

Xuemin (Sherman) Shen (Fellow, IEEE) received the Ph.D. degree in electrical engineering from Rutgers University, New Brunswick, NJ, USA, in 1990.

He is currently a University Professor with the Department of Electrical and Computer Engineering, University of Waterloo, Canada. He is also a registered Professional Engineer in ON, Canada. His research focuses on network resource management, wireless network security, the Internet of Things, 5G and beyond, and vehicular *ad hoc*, and sensor networks. He was a member of the IEEE Fellow Selection Committee of the ComSoc. He is an Engineering Institute of Canada Fellow, a Canadian Academy of Engineering Fellow, a Royal Society of Canada Fellow, a Chinese Academy of Engineering Foreign Member, and a Distinguished Lecturer of the IEEE Vehicular Technology Society and Communications Society. He received the R.A. Fessenden Award from IEEE, Canada, in 2019; the Award of Merit from the Federation of Chinese Canadian Professionals, ON, Canada, in 2019; the Technical Recognition Award from the Wireless Communications Technical Committee in 2019; the James Evans Avant Garde Award from the IEEE Vehicular Technology Society in 2018; the Education Award in 2017 and the Joseph LoCicero Award in 2015 from the IEEE Communications Society; the AHSN Technical Committee in 2013; the Excellent Graduate Supervision Award from the University of Waterloo in 2006; and the Premier's Research Excellence Award (PREA) from the Province of Ontario, Canada, in 2003. He served as the Technical Program Committee Chair/Co-Chair for IEEE Globecom'16, IEEE Infocom'14, IEEE VTC'10 Fall, and IEEE Globecom'07, and the Chair for the IEEE Communications Society Technical Committee on Wireless Communications. He was the Vice President for the Technical and Educational Activities and Publications; a Member-at-Large on the Board of Governors; and the Chair of the Distinguished Lecturer Selection Committee. He is also the President Elect of the IEEE Communications Society. He served as the Editor-in-Chief for IEEE INTERNET OF THINGS JOURNAL, *IEEE Network*, and *IET Communications*.